Pandey, V.; Van Dooren, S.; Ritzmann, J.; Pla Moreno, B.; Onder, C. (2021). Variable smoothing of optimal diesel engine calibration for improved performance and drivability during transient operation. International Journal of Engine Research. 22(6):1888-1895. https://doi.org/10.1177/1468087420918801

Variable Smoothing of Optimal Diesel Engine Calibration for Improved Performance and Drivability during Transient Operation

Varun Pandey[1] , Stijn van Dooren[2] , Johannes Ritzmann[2] , Benjamín Pla[1] , Christopher Onder[2]

Abstract

The model based method to define the optimal calibration maps for important Diesel engine parameters may involve three major steps. First, the engine speed and load domain—in which the engine is operated—is identified. Then, a global engine model is created, which can be used for offline simulations to estimate engine performance. Finally, optimal calibration maps are obtained by formulating and solving an optimisation problem, with the goal of minimizing fuel consumption while meeting constraints on pollutant emissions. This last step in the calibration process usually involves smoothing of the maps in order to improve drivability. This article presents a method to trade off map smoothness, brake specific fuel consumption (BSFC), and nitrogen oxides $\mathrm{NO_x}$ emissions. After calculating the optimal but potentially non-smooth calibration maps, a variation-based smoothing method is employed to obtain different levels of smoothness by adapting a single tuning parameter. The method was experimentally validated on a heavy-duty Diesel engine, and the non-road transient cycle (NRTC) was used as a case study. The error between the reference and actual engine torque was used as a metric for drivability, and the error was found to decrease with increasing map smoothness. After having obtained this trade-off for various fixed levels of smoothness, a time-varying smoothness calibration was generated and tested. Experimental results showed that, with a time-varying smoothness strategy, $\mathrm{NO_x}$ emissions could be reduced by 4%, while achieving the same drivability and fuel consumption as in the case of a fixed smoothing strategy.

Keywords

Diesel engine calibration; calibration map smoothing; drivability; $\mathrm{NO_x}$ emissions; variable smoothing

Introduction

The control structure of modern Diesel engines consists of feedforward and feedback controllers. Fixed look-up tables, commonly referred to as calibration maps, are employed in the setpoint generator and feedforward controllers [1,2]. The goal of engine calibration is to obtain optimal and smooth maps. The article by Castagne et al.[3] gives an overview of several calibration methods. The authors explain traditional local approaches, characterised by a phase of smoothing after local optimal settings are found, as well as global approaches, which directly include engine speed and load parameters in the engine model. In the article by Arya et al.[4], the authors propose an automated smooth calibration generation method, which is a subset of the global approach and shows improvements in engine performance and map smoothness.

The process of model-based engine calibration has been broadly divided into three steps by the authors in[5,6]. The first step is to select steady-state operating points which are representative of the engine operation. Then, a global engine model is developed and validated using measurement data from steady-state experiments. Finally, optimisation and smoothing are carried out for a representative driving cycle, with the goal of minimizing fuel consumption, while meeting constraints on pollutant emission and ensuring good drivability.

The term drivability is often defined only qualitatively. Assis et al.[7] define drivability as the capability of the engine to deliver the torque requested by the driver in a way which is pleasant to the driver. From a vehicle perspective, the driver subjectively provides feedback regarding drivability during the vehicle development phase. Pedal tip-in and tip-out are the typical drivability testing scenarios. The authors show that, even though the torque produced by the engine is desired to be equal to that demanded by the driver, it may result in undesirable behaviour due to powertrain excitation's during large torque steps. The authors propose a rail pressure control strategy to dampen the impact of sudden jumps in the engine torque. Nessler et al.[8] define drivability as the transition felt by the driver between engine speed and load points during real vehicle driving, which means that

[1]CMT–Motores Térmicos, Universitat Politècnica de València, Valencia, Spain
[2]Swiss Federal Institute of Technology (ETH), Zurich, Switzerland

Corresponding author:
Varun Pandey, CMT–Motores Térmicos, Universitat Politècnica de València, Camino de Vera Sn, E-46022 Valencia, Spain
Email: vapan2@mot.upv.es

a constant power supply is necessary during acceleration phases while avoiding sudden reduction of torque in order to have a good drivability. The authors propose to reduce the gaussian curvature of the optimal calibration maps in order to obtain smoother maps. In the articles by Nishio et al.[9] and Niedernolte et al.[10], a constraint in the step size for each parameter is applied to generate drivable calibration maps. However, some loss of optimality has been shown by the authors in terms of engine performance due to the manual elimination of the peaks in the map. This method requires all other parameters to be adjusted in a consistent way in order to achieve the target torque. However, no relationship has been shown between map smoothing on the torque reference following capability and the engine performance.

From an engine perspective, other than calibration map smoothing, some transient compensation strategies are also applied in[11] in order to obtain smooth transients, which in fact is another method of improving drivability. Adaptation of exhaust-gas recirculation (EGR) and fuel injection has an impact on transient emissions and drivability, as shown in the article by Zentner et al.[12]. The authors propose an EGR and injection limiter to reduce $\mathrm{NO_x}$ emissions and to improve drivability and the drivability was characterised by the transient response of the engine during load steps.

This article presents a single tuning parameter for the trade-off between fuel consumption, $\mathrm{NO_x}$ emissions and drivability during transient engine operation. Drivability is addressed as the capability of the engine to follow a reference torque profile. A model-based optimal calibration approach is used to obtain maps which meet a specified $\mathrm{NO_x}$ emissions limit while minimizing the fuel consumption. Then, the tuning parameter is introduced to obtain different levels of map smoothness, which is based on the classical total variation method proposed by Rudin et al.[13] and has been extensively used in the literature[14,15]. Finally, a time-varying smoothness strategy is generated and tested, with the goal to further improve engine performance and drivability, as compared to calibration maps with a fixed level of smoothness. The main contributions of this article are:

- A variation-based methodology is proposed to change the smoothness of the calibration maps using a single tuning parameter. The additional degree of freedom can be used to trade off fuel consumption, $\mathrm{NO_x}$ emissions, and drivability. This flexibility can be of great help for the calibration engineer, while optimality is guaranteed at all times.
- A time-varying smoothness strategy is proposed to further improve engine performance and drivability. This is achieved by exploiting the fact that the driving cycle consists of various phases with the engine operation being more or less transient. By choosing an appropriate smoothing strategy for each phase, the $\mathrm{NO_x}$ emissions can be reduced, while having the same fuel consumption and drivability as in the case of a fixed smoothing strategy.

The paper is structured as follows: after introducing the experimental facility in section 2, the engine model and model-based calibration approach are described in section 3. In section 4, the proposed calibration map smoothing method is explained. Section 5 presents the experimental results that demonstrate the trade-off between engine performance and drivability. In section 6, the idea and experimental results of a time-varying smoothing strategy are presented. Finally, the work is concluded in the last section.

Type	Heavy-duty Diesel engine
Technical data	7 litres, 4 cylinders
Rated power	200 kW @ 1900 rpm
Features	Common rail fuel injection, turbocharged, cooled EGR

Table 1. Engine characterstics

Experimental Facility

The measurements presented in this study were obtained from a dynamic engine test-bench at ETH Zurich. The engine under consideration is a commercial heavy-duty Diesel engine. Its main characteristics are listed in Table 1. Naturally, the methodology presented in this paper is not limited to this engine, but might be applied to any engine configuration. For the rapid prototyping of the software developed and tested in this study, a dSPACE MicroAutoBox system was applied in combination with MATLAB/Simulink from MathWorks, Inc. This device is also used for the data acquisition of the various sensor signals. The engine speed is controlled by a highly dynamic dynamometer which allow for fast control of the rotational speed. With a maximum torque of 1100 Nm, and a rotational inertia of 0.9 kgm^2, the maximum angular acceleration equals 1222 rad/s^2 or 11670 rpm/s. This is more than sufficient to accurately track a transient engine speed setpoint/trajectory such as that of the NRTC. Therefore, the engine speed can be considered an exogenous input rather than an output of the system.

Engine Model and Model-based Calibration

For the calibration of Diesel engines, it is common practice to model the input-output relationships statically[16,17]. Various software tools are available to support the calibration engineer with the steady-state measurements and subsequent modelling[18–20]. After that, model-based optimisation techniques are often used to find an engine calibration that yields the lowest possible fuel consumption while adhering to the limits on pollutant emissions[21,22].

For the engine in this study, the static engine model and model-based calibration were obtained as described in [23]. The control inputs u consist of the amount of fuel injected per cylinder and per cycle m_{inj}, the start-of-injection u_{soi} in degrees before top dead centre, and the desired burned gas ratio x_{bg} in the intake manifold. Whilst the amount of injected fuel is controlled to reach the requested torque T_e^{ref}, the two remaining control inputs u_{soi} and x_{bg} are the degrees of freedom to trade off fuel consumption $\dot{m}_f$ against engine-out $\mathrm{NO_x}$ emissions $\dot{m}_{\mathrm{NO_x}}$. This is done as in[24] by formulating and solving the following optimisation problem:

$$u^*(\omega_e, T_e, \mu_{\mathrm{NO_x}}) = \arg\min_u \{(1-\mu_{\mathrm{NO_x}})\cdot \dot{m}_f + \mu_{\mathrm{NO_x}} \cdot \dot{m}_{\mathrm{NO_x}}\} \quad (1)$$

The optimal control inputs u^* for each engine operating point depend on the weighting or strategy parameter $\mu_{\mathrm{NO_x}} \in$

$[0, 1]$. Choosing a higher value for $\mu_{\mathrm{NO_x}}$ results in lower engine-out $\mathrm{NO_x}$ emissions, but at the cost of a higher fuel consumption. While the engine strategy can—and usually is—fixed during the calibration process, the authors of[24,25] have shown that an adaptive operating strategy can be used to adapt the raw emissions in a situation-specific manner.

The optimal values from (1) are stored on the engine control unit (ECU) as static maps that serve as a feedforward controller. An EGR controller controls the intake valve and EGR valve position to reach the desired burned gas ratio.

Variable Map Smoothing

The optimal calibration maps obtained from the previous section are usually non-smooth. The calibration engineer may chose to smooth them manually or using available tools as in[18–20]. The methods are usually based on filtering techniques, where the value of the filtered data point is the average of the original data point and its adjacent points. A group of adjacent points in the original data are multiplied point-by-point by a set of coefficients that defines the smooth shape, the products are added up and divided by the sum of the coefficients, which becomes one point of smoothed data. Subsequently, the set of coefficients is shifted one point down the original data and the process is repeated. Mean filtering methods are not well suited for specifically eliminating peaks from the maps. Another method used for smoothing is based on computing the second derivative (local curvature) at each point and then calculating the average of the squared values of the local curvature for the entire map.

The methods described above do not explicitly take into account the cost of smoothing in terms of closeness to the original map or the loss of optimality, but it is a common practice to iterate these processes to minimize loss of optimality. In this article, a variational method is applied to obtain smooth maps. The method is based on a classical variation model for image denoising, originally proposed by Rudin et al. in[13]. The problem has been formulated as the following convex optimisation problem and solved by the primal-dual method as demonstrated by Zhi et al. in[14]:

$$\min_{u} \int \{ \, (1 - \mu_{sm}) \cdot (u - u^*)^2 + \mu_{sm} \cdot \nabla u_{x,y} \, \} \, dx \, dy \tag{2}$$

where u are the control inputs of the smoothed two-dimensional (x,y) calibration map and u^* denotes the optimal but non-smooth map, obtained from the model-based calibration method described in the previous section. For all the investigations presented in this article, a fixed engine strategy $\mu_{\mathrm{NO_x}} = 0.11$ was used.

The first term in (2) accounts for the closeness of the obtained smoothed map to the original optimal but generally non-smooth map, and the second term contributes to the total variation of the obtained map. The closeness to the original map has been considered rather than the cost in terms of fuel consumption and $\mathrm{NO_x}$ emissions in (2). This is done to separate the optimisation and smoothing phases in the calibration process. The normalised total variation in the direction of engine speed and torque is $\nabla u_{x,y}$. The regularisation weight $\mu_{sm} \in [0, 1]$ is used to tune the smoothness level of the maps. When $\mu_{sm} = 1$, only the second term in (2) is minimised, producing the smoothest possible map. For $\mu_{sm} = 0$, no smoothing is applied, and the resulting map is the original non-smooth map.

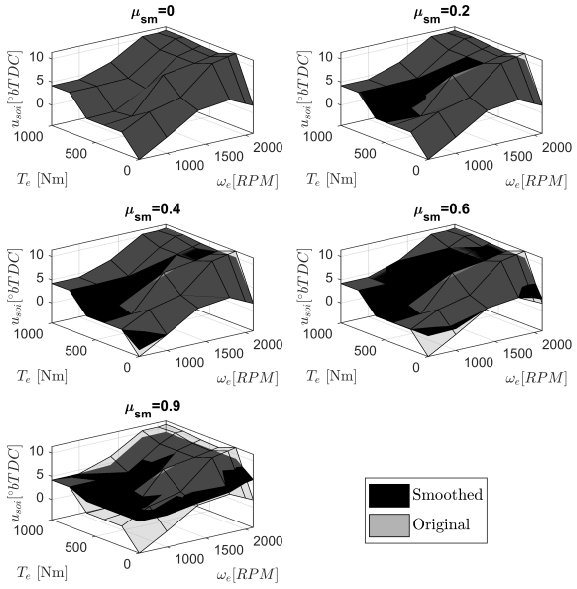

Figure 1. Impact of smoothing on soi calibration maps

The continuous problem (2) can be discretised and solved numerically as in (3), where $n = 5$ is the grid size of the map under consideration:

$$\min_{u} \sum_{i=1}^{n} \sum_{j=1}^{n} \{ \, (1 - \mu_{sm}) \cdot (u_{i,j} - u^*_{i,j})^2 + \mu_{sm} \cdot \nabla u_{i,j} \, \} \tag{3}$$

in which $\nabla u_{i,j}$ denotes the first order forward difference operation, defined as:

$$\nabla u_{i,j} = \begin{bmatrix} u_{i+1,j} - u_{i,j} \\ u_{i,j+1} - u_{i,j} \end{bmatrix} \tag{4}$$

Five calibration maps with different values of $\mu_{sm} \in \{0, 0.2, 0.4, 0.6, 0.9\}$ were calculated. Figures 1 and 2 show the impact of varying μ_{sm} on the calibration maps for start-of-injection (u_{soi}) and burned gas ratio x_{bg}, respectively. The original maps u^* are shown in grey and can be considered non-smooth. With increasing value of μ_{sm}, the smoothness of the maps visibly increases. As μ_{sm} is increased from zero, the maps initially get smoother where a maximum reduction of the total variation can be achieved. When μ_{sm} is further increased, also the remaining regions of the map become smoother.

In Figure 3, the impact of μ_{sm} on the primary and secondary terms of (3) is shown. As expected, with increasing μ_{sm}, the normalised total variation of the map decreases at the cost of its distance from the original map.

Trade-off between Performance and Drivability

The calibration maps in Figures 1 and 2 show that with an increasing μ_{sm}, the start-of-injection (SOI) is advanced at

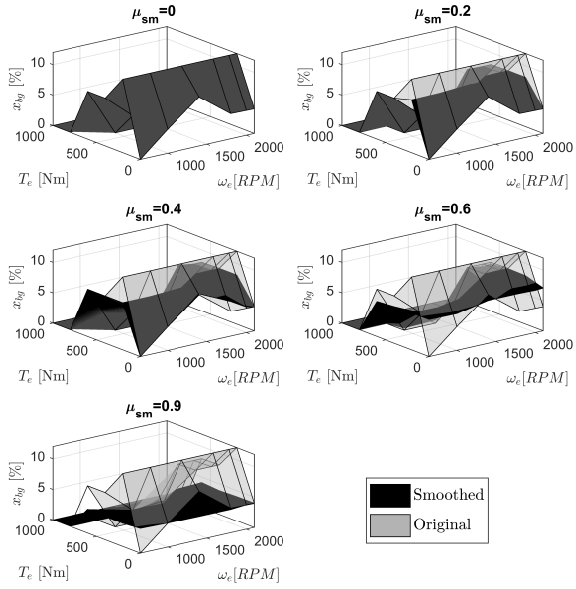

Figure 2. Impact of smoothing on egr calibration maps

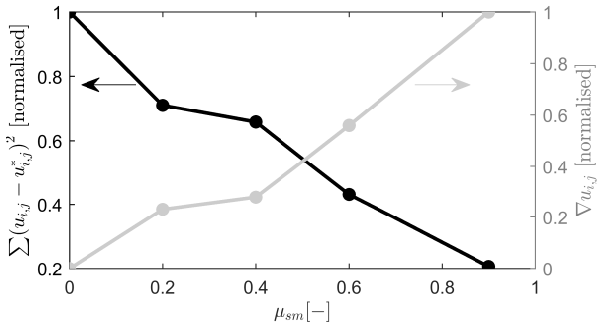

Figure 3. Impact of weigting factor on the total variation $\nabla u_{i,j}$ and distance from the original map $\sum(u_{i,j} - u^*_{i,j})^2$ for x_{bg}

lower engine speeds and torque, whereas SOI is retarded at higher engine speed and torque. On the other hand, the burned gas ratio is reduced at high engine torque and increased for $\mu_{sm} = 0.6$ and 0.8, regardless of the engine speed. The obtained calibration maps are stored on the ECU as static maps to serve as a feedforward controller. Taking the NRTC as a case study, the various maps are implemented and tested on the engine test-bench. The results are presented and discussed in this section.

Figure 4 shows the instantaneous engine torque, start-of-injection, burned gas ratio, fuel consumption, and $\mathrm{NO_x}$ emissions during the NRTC. The cumulative impact of the control actions can be clearly seen in the instantaneous $\mathrm{NO_x}$ emissions in the bottom plot.

In order to compare the torque response of each calibration map, the error between the reference and actual engine torque is calculated for the cycle as:

$$T_e^{\text{error}} = \sum_{\text{NRTC}} (T_e^{\text{ref}} - T_e)^2 \tag{5}$$

The top plot in Figure 5 shows the reference torque profile T_e^{ref}. In the bottom plot, the normalised T_e^{error} is shown for the cycle. It is normalised by dividing T_e^{error} obtained with a specific calibration by the error obtained with $\mu_{sm} = 0$. As expected, with increasing smoothness of the calibration maps, the torque error is reduced in a consistent manner.

μ_{sm}	0	0.2	0.4	0.6	0.9
BSFC	0.991	0.99	0.989	0.992	1
$\mathrm{NO_x}$	0.916	0.938	0.977	0.979	1
$\mathrm{T_{error}}$	1	0.977	0.955	0.943	0.917

Table 2. Impact of μ_{sm} on BSFC (normalised), $\mathrm{NO_x}$ emissions (normalised) and T_e^{error} for NRTC

In Figure 6, the trade-off between fuel consumption, $\mathrm{NO_x}$ emissions, and torque error is shown. For $\mu_{sm} = 0.9$, the $\mathrm{NO_x}$ emissions increase by 9%, fuel consumption increases by 1%, and an improvement in torque response is observed. Table 2 consolidates the parameters related to the engine performance with different values of μ_{sm}. Based on this data, the calibration engineer may chose the value of μ_{sm} that fulfils the performance requirements.

Time-varying Smoothness Calibration

A map smoothing method was developed and used to obtain a trade-off between fuel consumption, $\mathrm{NO_x}$ emissions and T_e^{error} in the previous section. Based on the resulting trade-off, a time-varying smoothness strategy is proposed to minimise the $\mathrm{NO_x}$ emissions while constraining fuel consumption and T_e^{error}. A case study is designed to assess the impact of time-varying smoothness on the engine performance. From the set of five calibrations of the previous section, $\mu_{sm} = 0.2$ is assumed to be the favourable choice of a calibration engineer based on the emission and the drivability constraints. At this setting, the engine $\mathrm{NO_x}$ emissions increase only by 1-2% while having similar BSFC and 3% reduction in torque error compared to the optimal maps. The objective of the case study is to obtain a sequence of μ_{sm} for the NRTC to minimise $\mathrm{NO_x}$ emissions while obtaining the same or less fuel consumption and torque error as compared to the fixed smoothness strategy. To do this, μ_{sm} is adapted in a time window of 100 s. In each time window, μ_{sm} is selected from the already tested set of calibrations such that the cumulative $\mathrm{NO_x}$ emissions in the window are minimised while keeping fuel consumption and T_e^{error} less than or equal to the reference calibration, which is $\mu_{sm} = 0.2$. This can be formulated as the following optimisation problem:

$$\begin{aligned} \min_{\mu_{sm}} \quad & \sum_{win} \mathrm{NO_x} \\ \text{subject to} \quad & \sum_{win} \dot{m}_f \leq \sum_{win} \dot{m}_f(\mu_{sm} = 0.2) \\ & \sum_{win} T_e^{\text{error}} \leq \sum_{win} T_e^{\text{error}}(\mu_{sm} = 0.2) \end{aligned} \tag{6}$$

where $win = 100$ s is the size of the time window, during which the performance parameters are cumulated and based on which the smoothing strategy is chosen. The resulting time-varying calibration, i.e. sequence of μ_{sm}, is tested on the engine test-bench on the NRTC.

The strategy obtained from (6) is shown in the top plot in Figure 7. The normalised engine torque errors obtained

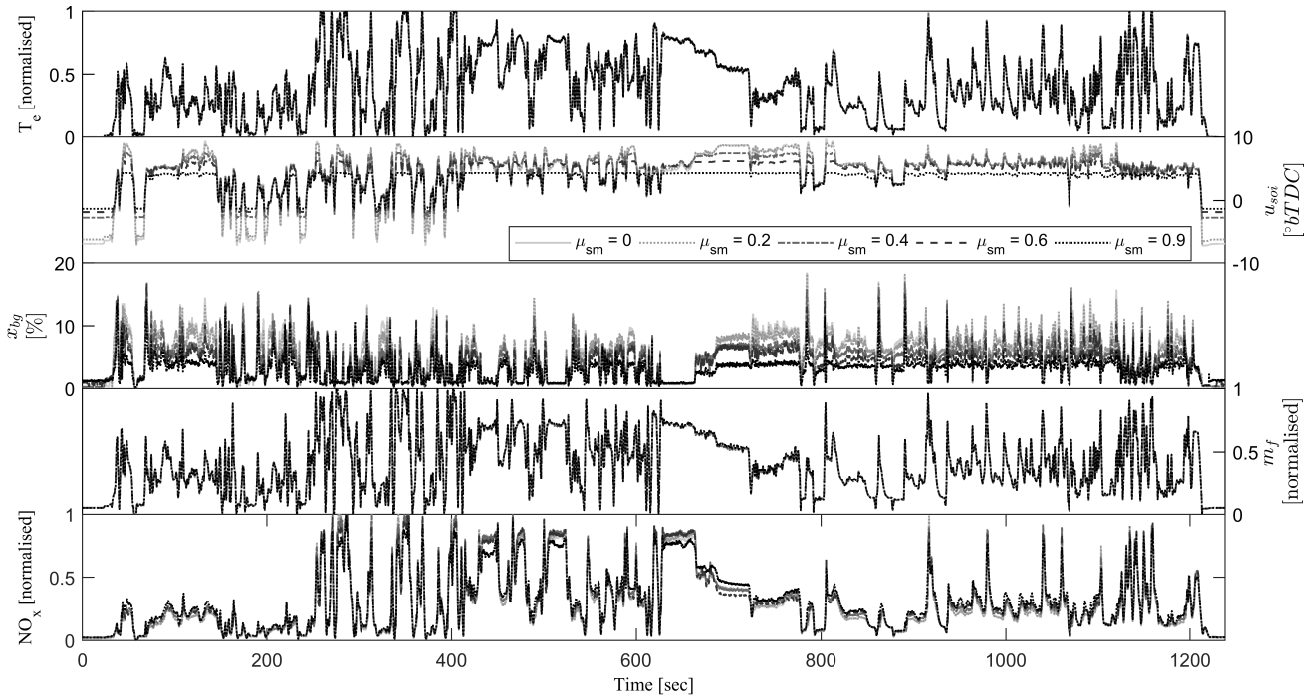

Figure 4. Instantaneous engine torque, start-of-injection, burnt gas ratio, fuelling rate, $\mathrm{NO_x}$ emissions measured at the test bench with different smoothness levels

from the fixed and time-varying strategies are shown in the bottom plot. The control actions and instantaneous engine performance are compared for the two strategies in Figure 8. The $\mathrm{NO_x}$ emissions are largely reduced from 300 to 500 s, with similar fuel consumption and improved drivability. From 600 to 900 s, with $\mu_{sm} = 0$, the calibration is optimal in terms of fuel consumption and $\mathrm{NO_x}$ emissions. The non-smooth maps have less impact on the drivability, as the driving cycle is largely non-transient during this time period.

For the purpose of analysis, the cycle can be divided into four distinct phases, based on engine speed, torque, and the amount of transient operation. The first phase ranges from 0 to 250 s and consists of medium load and medium transients, phase 2 is between 250 to 450 s consisting of high load and high transients, the third phase is between 450 to 900 s consisting of high load and low transients, and phase 4 is between 900 to 1238 s and has low load and medium transients.

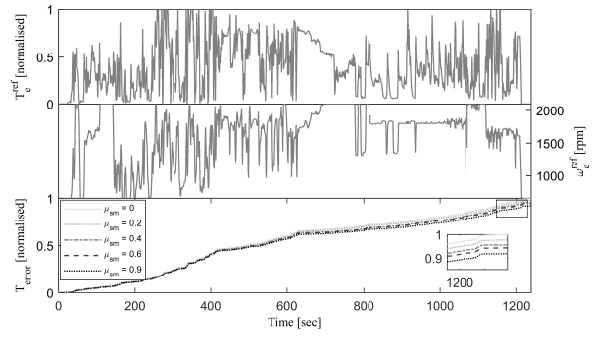

Figure 5. Reference torque profile (top), reference speed profile (middle) and cumulative error in torque reference tracking (bottom)

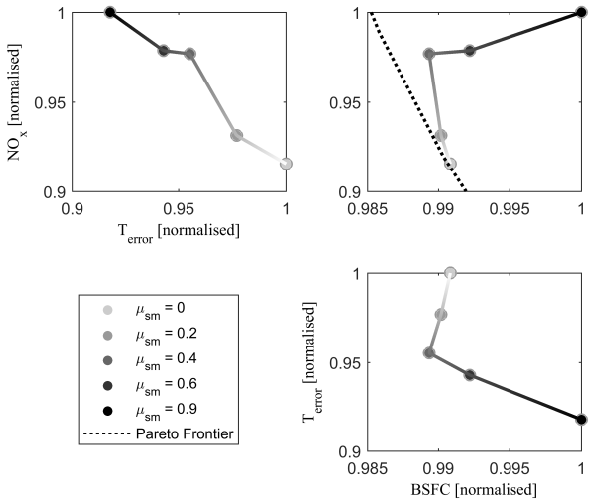

Figure 6. Trade-off between torque error and engine performance with different smoothing levels

Phase 1: With increased smoothness, x_{bg} is decreased and u_{soi} remains largely unaffected. Resulting in higher $\mathrm{NO_x}$ emissions with higher μ_{sm}. Therefore, the controller choses to operate at $\mu_{sm} = 0.2$.

Phase 2: With higher map smoothness, x_{bg} is reduced while u_{soi} is significantly retarded, resulting in reduced $\mathrm{NO_x}$ emissions. On the other hand, reducing x_{bg} has a positive impact on torque reference following capability of the engine. During high load transients, the fuel injection is temporarily reduced to avoid high soot emissions[26]. This negatively influences the torque reference following capability. Therefore, a smooth actuation of x_{bg} and u_{soi} is desirable during this period. Another factor which positively

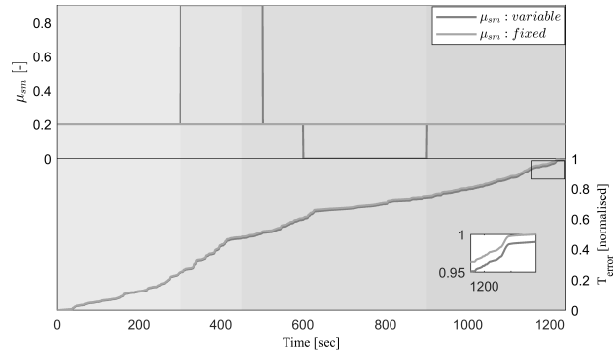

Figure 7. Top plot comparision of variable calibration smoothing and fixed calibration for NRTC cycle; bottom plot is the cumulative error in torque reference following, the shade gets darker from phase 1 to phase 4 of the cycle

influences torque reference following capability is the improved acceleration of the turbocharger with reduced x_{bg} during load jumps. The controller increases μ_{sm} to 0.9, resulting in reduced $\mathrm{NO_x}$ emissions and improved torque reference following capability of the engine.

Phase 3: With increasing smoothness, u_{soi} is retarded compared to the original maps. The $\mathrm{NO_x}$ emissions are reduced as seen in the bottom plot of 8 at high loads where x_{bg} is zero. The controller chooses $\mu_{sm} = 0$ because the engine operation is less transient during this phase.

Phase 4: For medium loads at the end of the cycle, the x_{bg} and u_{soi} are more or less similar for all levels of smoothness. Therefore, the differences are minimal in the engine performance and thus $\mu_{sm} = 0.2$ is chosen.

Figure 9 shows the engine performance obtained with the time-varying smoothness strategy, as compared to the fixed calibration strategy. With the time-varying smoothness, $\mathrm{NO_x}$ emissions can be reduced by 3-4% compared to the fixed calibration, while maintaining the same fuel consumption and torque reference following capability.

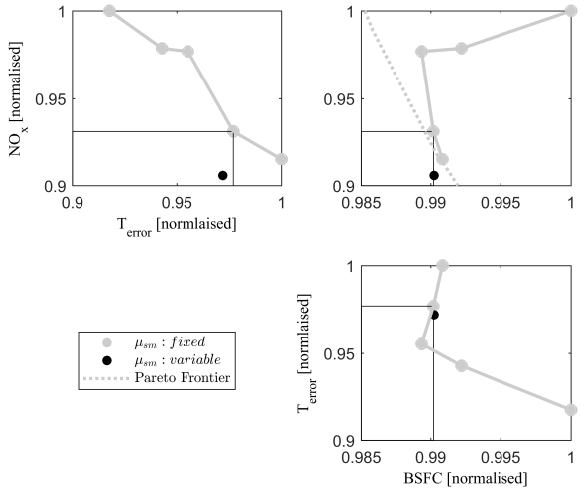

Figure 9. Comparison of engine performance for fixed and time-varying smoothness calibration

The result highlights the potential of variable smoothing on a driving cycle. Although, this demonstration is made for the NRTC it can be implemented in a prototyping system in real-time to emulate the real world scenario by online estimation of the error in torque, BSFC and $\mathrm{NO_x}$ emission. These estimations require a driving cycle prediction tool, an engine model and a supervisory controller to chose the optimal value of the proposed tuning parameter in real driving condition.

Summary and Conclusions

Drivability is improved by smoothing of optimal calibration maps obtained from model-based calibration. With smoothing of the calibration, the maps move away from the optimal settings. This results in a loss in optimality in terms of fuel consumption and $\mathrm{NO_x}$ emissions. This intervention is necessary especially during high transient engine operation, where a rough transition leads to poor drivability. A method is proposed to smoothen optimal calibration maps which are obtained from a model-based Diesel engine calibration approach. The optimal non-smooth maps, x_{bg} and u_{soi} minimises the fuel consumption while constraining the $\mathrm{NO_x}$ emissions for the NRTC. The smoothing method uses a tuning parameter μ_{sm} to reduce the total variation of the optimal maps to generate a set of smooth calibration maps. Drivability is addressed as the capability of the engine to follow the demanded torque profile and is shown to improve with the map smoothness. A trade-off between fuel consumption, $\mathrm{NO_x}$ emissions and torque error is obtained on the NRTC. Based on the results, an increase in μ_{sm} from 0 to 0.9 results in 9% increase in the $\mathrm{NO_x}$ emissions, 1% increase in fuel consumption and 9% decrease in T_e^{error}. A time varying smoothing method is proposed which adapts μ_{sm} in a moving time window based on the cumulative fuel consumption, the $\mathrm{NO_x}$ emissions and the torque error. In different phases of the cycle, the engine operates at different transient intensities. Having a degree of control freedom in map smoothness provide flexibility to adapt μ_{sm} based on the intensity of the transients. It has been demonstrated that same levels of torque reference tracking performance and fuel consumption can be achieved while reducing $\mathrm{NO_x}$ emissions by 3-4% with the application of time-varying smoothness strategy as compared to the state-of-the-art fixed calibration method.

An additional degree-of-freedom has provided more flexibility to control the engine with the time-varying smoothness strategy. The proposed method can be extended to the real world scenario by including a driving cycle prediction model, an engine model and a controller that can optimally choose the proposed smoothness tuning parameter such that the fuel-efficiency is maximised while limiting the reference torque error and the $\mathrm{NO_x}$ emission.

References

1. Lapuerta M, Ramos Á, Rubio S et al. Optimization of a diesel engine calibration for operating with a residual glycerol-derived biofuel. *International Journal of Engine Research* 2019; : 146808741989153DOI:10.1177/1468087419891535.
2. Yamasaki Y, Ikemura R and Kaneko S. Model-based control of diesel engines with multiple fuel injections. *International*

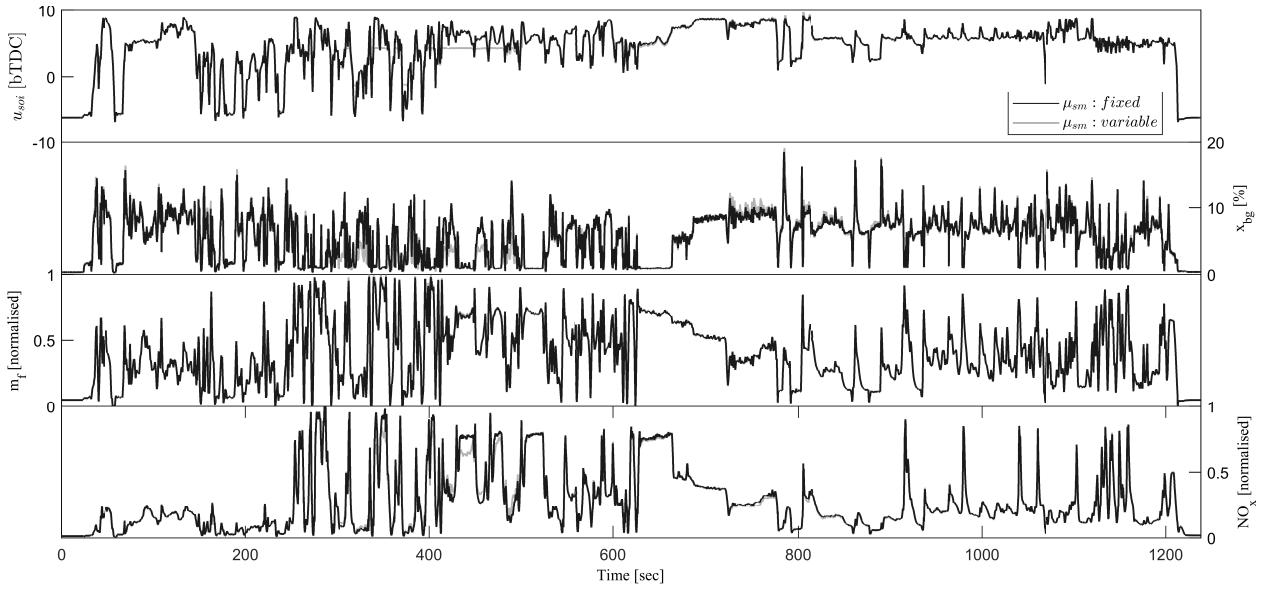

Figure 8. Performance trade-off comparison between fixed and variable smoothing method

Journal of Engine Research 2017; 19(2): 257–265. DOI: 10.1177/1468087417747738.

3. Castagné M, Bentolila Y, Chaudoye F et al. Comparison of engine calibration methods based on design of experiments (DoE). *Oil & Gas Science and Technology - Revue de IFP* 2008; 63(4): 563–582. DOI:10.2516/ogst:2008029.
4. Arya P, Millo F and Mallamo F. A fully automated smooth calibration generation methodology for optimization of latest generation of automotive diesel engines. *Energy* 2019; 178: 334–343. DOI:10.1016/j.energy.2019.04.122.
5. Langouët H, Métivier L, Sinoquet D et al. Engine calibration: multi-objective constrained optimization of engine maps. *Optimization and Engineering* 2011; 12(3): 407–424. DOI: 10.1007/s11081-011-9140-8.
6. Park S, Kim Y, Woo S et al. Optimization and calibration strategy using design of experiment for a diesel engine. *Applied Thermal Engineering* 2017; 123: 917–928. DOI:10.1016/j.applthermaleng.2017.05.171.
7. Assis EMD, Kurauchi R, Carloti MC et al. Drivability improvements on electronic diesel engines. In *SAE Technical Paper Series*. SAE International. DOI:10.4271/2003-01-3656.
8. Nessler A, Haukap C and Roepke K. Global evaluation of the drivability of calibrated diesel engine maps. In *2006 IEEE Conference on Computer Aided Control System Design, 2006 IEEE International Conference on Control Applications, 2006 IEEE International Symposium on Intelligent Control*. IEEE. DOI:10.1109/cacsd-cca-isic.2006.4777063.
9. Nishio Y, Murata Y, Yamaya Y et al. Optimal calibration scheme for map-based control of diesel engines. *Science China Information Sciences* 2018; 61(7): 70205. DOI:10.1007/s11432-017-9381-6.
10. Niedernolte H, Klopper F, Mitterer A et al. Workflow for data evaluation during basic calibration of combustion engines. In *2006 IEEE Conference on Computer Aided Control System Design, 2006 IEEE International Conference on Control Applications, 2006 IEEE International Symposium on Intelligent Control*. IEEE. DOI:10.1109/cacsd-cca-isic.2006.4776957.
11. Zhou X, Liu E, Sun D et al. Study on transient emission spikes reduction of a heavy-duty diesel engine equipped with a variable intake valve closing timing mechanism and a two-stage turbocharger. *International Journal of Engine Research* 2018; 20(3): 277–291. DOI:10.1177/1468087417748837.
12. Zentner S, Schfer E, Onder C et al. Model-based injection and egr adaptation and its impact on transient emissions and drivability of a diesel engine. *IFAC Proceedings Volumes* 2013; 46(21): 89–94. DOI:10.3182/20130904-4-jp-2042.00124.
13. Rudin LI, Osher S and Fatemi E. Nonlinear total variation based noise removal algorithms. *Physica D: Nonlinear Phenomena* 1992; 60(1-4): 259–268. DOI:10.1016/0167-2789(92)90242-f.
14. Zhi Z, Shi B and Sun Y. Primal-dual method to smoothing TV-based model for image denoising. *Journal of Algorithms & Computational Technology* 2016; 10(4): 235–243. DOI: 10.1177/1748301816656298.
15. Aubert G and Kornprobst P. *Mathematical Problems in Image Processing*. Springer New York, 2006. DOI:10.1007/978-0-387-44588-5.
16. Berger B. *Modeling and Optimization for Stationary Base Engine Calibration*. PhD Thesis, TECHNISCHE UNIVERSITAT MUNCHEN, 2012.
17. Schler M. *Stationre Optimierung der Motorsteuerung von PKW-Dieselmotoren mit Abgasturbolader durch Einsatz schneller neuronaler Netze*. PhD Thesis, TU Darmstadt, 2001.
18. Gschweitl K, Pfluegl H, Fortuna T et al. Increasing the efficiency of model-based engine applications through the use of CAMEO online DoE toolbox. *ATZ worldwide* 2001; 103(7-8): 17–20. DOI:10.1007/bf03226800.
19. Gutjahr T, Kruse T and Huber T. Advanced modeling and optimization for virtual calibration of internal combustion engines.
20. The MathWorks, Inc. *MathWorks Model-Based Calibration Toolbox - CAGE Users Guide. ., 2017*, 2017.
21. Hafner M and Isermann R. Multiobjective optimization of feedforward control maps in engine management systems towards low consumption and low emissions. *Transactions of the Institute of Measurement and Control* 2003; 25(1): 57–74.

DOI:10.1191/0142331203tm074oa.
22. Sequenz H. *Emission Modelling and Model-Based Optimisation of the Engine Control*. PhD Thesis, Technischen Universitat Darmstadt, 2013.
23. van Dooren S, Balerna C, Salazar M et al. Optimal diesel engine calibration using convex modelling of pareto frontiers. *Control Engineering Practice* 2020; 96: 104313. DOI:10.1016/j.conengprac.2020.104313.
24. Elbert P, Amstutz A and Onder C. Adaptive control for the real driving emissions of diesel engines. *MTZ worldwide* 2017; 78(12): 68–74. DOI:10.1007/s38313-017-0127-5.
25. Guardiola C, Pla B, Bares P et al. Adaptive calibration for reduced fuel consumption and emissions. *Proceedings of the Institution of Mechanical Engineers, Part D: Journal of Automobile Engineering* 2016; 230(14): 2002–2014. DOI: 10.1177/0954407016636977.
26. Guzzella L and Amstutz A. Control of diesel engines. *IEEE Control Systems* 1998; 18(5): 53–71. DOI:10.1109/37.722253.

Acknowledgements

The authors acknowledge the support of Spanish Ministerio de Economia, Industria y Competitividad through project TRA2016-78717-R and This work was developed during the research stay of Varun Pandey at the ETH funded by the Programa de Movilidad para la Formacion de Personal Investigador del Vicerrectorado de Investigacion, Innovacion y Transferencia de la UPV.